



TITLE:

# Design Study of a Beam Matching Section for the ICR Proton Linac

AUTHOR(S):

Dewa, Hideki; Iwashita, Yoshihisa; Okamoto, Hiromi; Noda, Akira; Shirai, Toshiyuki; Inoue, Makoto

---

CITATION:

Dewa, Hideki ...[et al]. Design Study of a Beam Matching Section for the ICR Proton Linac. Bulletin of the Institute for Chemical Research, Kyoto University 1992, 70(1): 89-98

ISSUE DATE:

1992-03-30

URL:

<http://hdl.handle.net/2433/77429>

RIGHT:

## Design Study of a Beam Matching Section for the ICR Proton Linac

Hideki DEWA\*, Yoshihisa IWASHITA\*, Hiromi OKAMOTO\*,  
Akira NODA\*, Toshiyuki SHIRAI\* and Makoto INOUE\*

*Received February 18, 1992*

A new beam matching system between the RFQ (Radio Frequency Quadrupole) linac and the DTL (Drift Tube Linac) is investigated. This system consists of four PMQ (Permanent Magnet Quadrupole) lenses and a double gap buncher which is a QWR (quarter wave-length resonator). The shunt impedance optimization of the buncher is studied by the SUPERFISH with the approximated geometry. The shunt impedance and Q-value of the new cold model are measured.

**KEY WORDS :** Beam matching/RF cavity/Buncher/PMQ/Quarter wave-length resonator/

### 1. INTRODUCTION

The ICR proton linac, whose operation frequency is 433.3 MHz, consists of the RFQ (Radio Frequency Quadrupole) linac and the Alvarez DTL (Drift Tube Linac). The RFQ linac accelerates 50 keV protons from the multi-cusp ion source up to the energy of 2 MeV, followed by the DTL whose output energy is 7 MeV.

The MEBT (Medium Energy Beam Transport) system, which is referred here as the section between the RFQ linac and the DTL, transports proton beams from the RFQ linac, achieving the beam matching to the acceptance of the DTL. A matching section using eight focusing magnets with a buncher has been reported in the previous work for the ICR proton linac.<sup>1)</sup> The shunt impedance of this first buncher is 0.43 M $\Omega$  per gap, which requires RF power of over 10 kW. Since the available power for the buncher is less than 10 kW, a new buncher with higher shunt impedance should be designed.

The major advantages of a quarter wave-length resonator (QWR) for the buncher application are its small size and high efficiency. The design studies of this type of cavities have been performed at many other laboratories.<sup>2)3)4)5)</sup> In the design study of our buncher, the parameters are optimized with the results from SUPERFISH<sup>6)</sup> calculation. The beam matching to the DTL acceptance is also calculated with the help of TRACE-3D<sup>7)</sup>. According to the SUPERFISH calculations, the requirement of the high shunt impedance makes the cavity size large. The old matching section design using eight PMQ (Permanent Magnet Quadrupole)

---

\* 出羽英紀, 岩下芳久, 岡本宏巳, 野田 章, 白井敏之, 井上 信: Nuclear Science Research Facility, Institute for Chemical Research, Kyoto University., Uji, Kyoto 611, Japan.

lenses should be modified to make enough space for the larger buncher cavity. We fabricate the cold model of the larger buncher to measure the shunt impedance and Q-value.

## 2. BEAM OPTICS CALCULATION

In order to match the beam ellipse parameters to the DTL acceptance, we calculate the phase space ellipse of the output beam from the RFQ linac with the PARMTEQ<sup>8)</sup> simulation, while the DTL acceptance is evaluated by the PARMILA<sup>9)</sup> simulation. Table 1 shows the phase space parameters of the output beam from the RFQ linac when the calculated unnormalized beam emittance of the input beam is  $100\pi$  mm mrad and the beam current is 60 mA. The phase space parameters of the DTL acceptance are shown in Table 2.

Transverse and longitudinal matching conditions is calculated with the computer code TRACE-3D. In our design, a transport system with four PMQ lenses and the double-gap buncher is studied, assuming that the buncher is placed around the middle of the 570 mm-long beam line between the RFQ linac and DTL.

At least four PMQ lenses are necessary to achieve the perfect matching because the field gradient and length of PMQs are fixed as shown in Table 3. The TRACE-3D automatically determines the positions of four PMQ lenses to match the phase space ellipses. From the results given in Fig. 1 and Table 4, transverse ellipses are almost matched within the 6 % error in the x-direction. This error is evaluated by

Table 1. The beam ellipse parameters at the end of the RFQ linac calculated by the PARMTEQ.

$\alpha x$	-1.494	$\beta x$	0.112 mm/mrad	$\varepsilon x$	$24.7\pi$ mm mrad
$\alpha y$	1.918	$\beta y$	0.145 mm/mrad	$\varepsilon y$	$28.4\pi$ mm mrad
$\alpha\phi$	0.092	$\beta\phi$	1.05 deg/keV	$\varepsilon\phi$	1990 deg keV

Table 2. The beam ellipse parameters of the DTL acceptance calculated by the PARMILA.

$\alpha x$	-2.359	$\beta x$	0.210 mm/mrad	$\varepsilon x$	$87\pi$ mm mrad
$\alpha y$	0.971	$\beta y$	0.0657 mm/mrad	$\varepsilon y$	$87\pi$ mm mrad
$\alpha\phi$	0.34	$\beta\phi$	0.269 deg/keV	$\varepsilon\phi$	4630 deg keV

Table 3. The specifications of the PMQ lenses used for our transport system.

Length	28.8 mm
Inner diameter	11 mm
Outer diameter	28 mm
Magnetic field gradient	18.8 kG/cm

# Design Study of a Beam Matching Section for the ICR Proton Linac

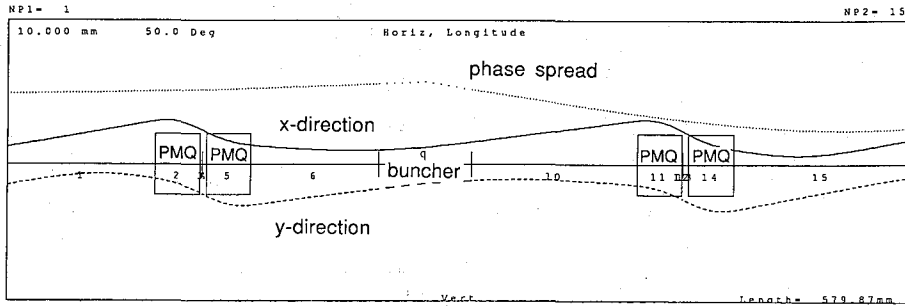


Fig. 1. The MEBT configuration optimized by TRACE-3D.

Table 4. The beam ellipse parameters at the entrance of the DTL calculated by the TRACE-3D. The TRACE-3D optimizes the positions of the four fixed-gradient PMQs to achieve the maximum matching to the DTL acceptance given in Table 2.

$\alpha_x$	-2.502	$\beta_x$	0.208 mm/mrad
$\alpha_y$	0.971	$\beta_y$	0.0657 mm/mrad
$\alpha_\phi$	0.341	$\beta_\phi$	0.269 deg/keV

$$\sqrt{\left(\frac{\alpha_x - \bar{\alpha}_x}{\bar{\alpha}_x}\right)^2 + \left(\frac{\beta_x - \bar{\beta}_x}{\bar{\beta}_x}\right)^2 + \left(\frac{\alpha_y - \bar{\alpha}_y}{\bar{\alpha}_y}\right)^2 + \left(\frac{\beta_y - \bar{\beta}_y}{\bar{\beta}_y}\right)^2 + \left(\frac{\alpha_\phi - \bar{\alpha}_\phi}{\bar{\alpha}_\phi}\right)^2 + \left(\frac{\beta_\phi - \bar{\beta}_\phi}{\bar{\beta}_\phi}\right)^2}$$

where the phase space parameters with bar indicate those of the DTL acceptance calculated with the PARMILA, and the other parameters correspond to the emittance of the output beam from the optimized MEBT designed with the TRACE-3D.

Perfect matching can not be found because of the fixed field gradient and the fixed length of the available PMQ lenses. According to the PARMILA simulation, the present solution, which includes the 6 %-mismatch, is permissible in the acceleration of proton beams without any particle loss in the DTL section.

For the longitudinal matching, the position and effective gap voltage of the buncher are optimized. It is concluded from the TRACE-3D calculations that the effective gap voltage of 116 kV is necessary for the longitudinal matching.

This matching solution is also confirmed by the PARMILA simulations with 3000 particles and the 100 % transmission rate is obtained as mentioned before. Figure 2 shows the transmission rate of the designed MEBT calculated by the PARMILA simulations at some specific values of the effective gap voltage.

The 70 kV effective gap voltage is necessary for zero-current beams, and 116 kV for 60 mA beams. The transmission rate of the MEBT without the buncher is 79.9 % at 0 mA and 62.4 % at 60 mA.

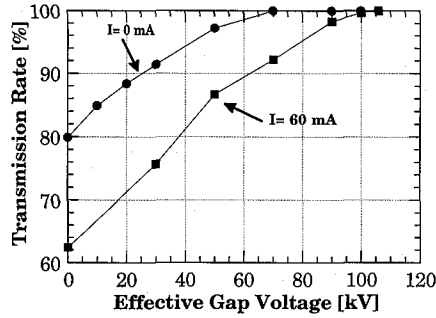


Fig. 2. The transmission rate of DTL as a function of effective gap voltage of buncher at  $I=0$  mA and  $I=60$  mA.

### 3. CAVITY DESIGN FOR THE BUNCHER

#### 3.1 The Design Method

A QWR cavity is adopted as our buncher cavity because of its good acceleration efficiency and the compact size. The resonant frequency of 433 MHz is the same as the RFQ linac and the DTL. The schematic view of the QWR buncher is shown in Fig. 3. The design parameters  $R$ ,  $r$ ,  $r_0$ ,  $L_c$ ,  $L_t$ ,  $L_g$ , are optimized to attain the maximum effective shunt impedance  $ZT^2$ , where  $Z$  and  $T$  are the shunt impedance and transit time factor, respectively.

The resonant frequency, the shunt impedance, the  $Q$  value, and the transit time factor of

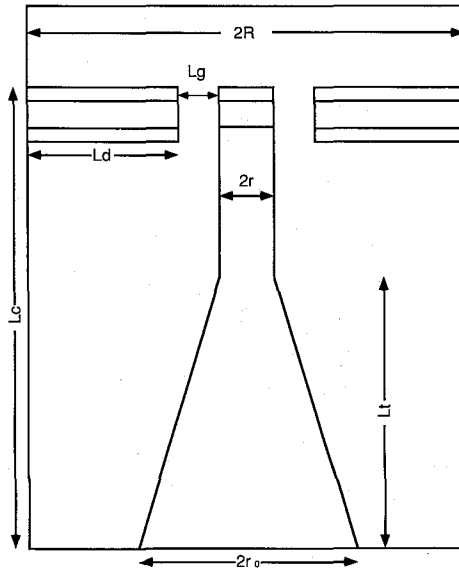


Fig. 3. The schematic view of QWR buncher.

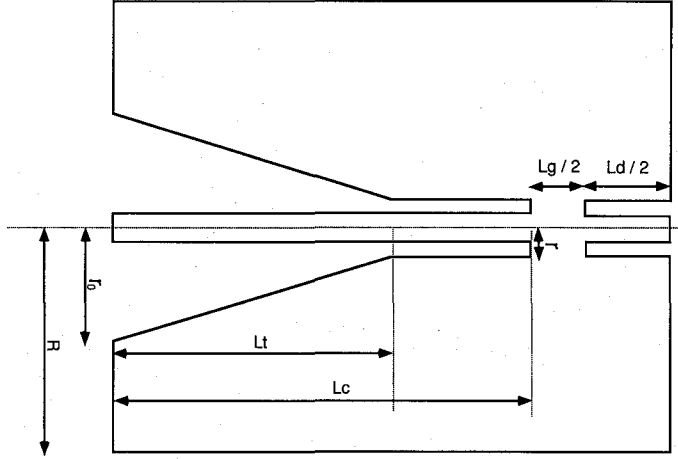


Fig. 4. The approximated axially-symmetric geometry of the buncher for the SUPERFISH calculation.

the buncher are calculated with the computer code SUPERFISH. The SUPERFISH can not be essentially applicable to such geometries as a QWR buncher, because it has no axial symmetry. To perform the buncher parameter optimization, we approximate it to axially-symmetric geometry shown in Fig. 4 for the SUPERFISH calculation. In this case,  $R$ ,  $r$ ,  $r_0$ , and  $L_t$ , are set at the same values as the real ones given in Fig. 3, but  $L_g$  and  $L_d$  must be chosen at the half values. This correction is necessary because the real buncher has two gaps and two noses.

### 3.2 The Calculation Results

Figure 5(a) shows the calculated shunt impedance based on the approximated symmetric geometry (Fig. 4). In these calculations, both  $r$  and  $L_g$  are fixed at 10 mm while we change the length of inner conductor,  $L_c$ , in order to adjust the resonant frequency at 433 MHz. The inner conductor is straight in the first stage of the SUPERFISH calculations. Larger  $R$  increases the shunt impedance. The available space on the beam line limits the  $R$  to be 80 mm.

The calculated shunt impedance as a function of the inner conductor radius  $r$  is shown in Fig. 5(b). The shunt impedance decreases as  $r$  increases from 5 mm to 20 mm.  $r$  is chosen to be 7 mm because of the additional consideration of the mechanical strength and the cooling water paths. The electric flux between inner and outer conductor is concentrated at the gap regions in this condition.

The advantage of a tapered inner conductor is confirmed with the SUPERFISH calculations, and  $r_0$  and  $L_t$  are optimized in the case where  $R=80$  mm and  $r=7$  mm. The  $r_0$  dependence on the shunt impedance is shown in Fig. 5(c) with the fixed  $L_t$  of 100 mm. The shunt impedance of the tapered cavity is 18 % larger than that of the untapered one. Figure 5 (d) shows the  $L_t$ -dependence of the calculated shunt impedance when  $r_0$  is fixed at 30 mm. The optimized value of  $L_t$  is 9.4 cm and that of  $r_0$  is 3 cm, as indicated by the results

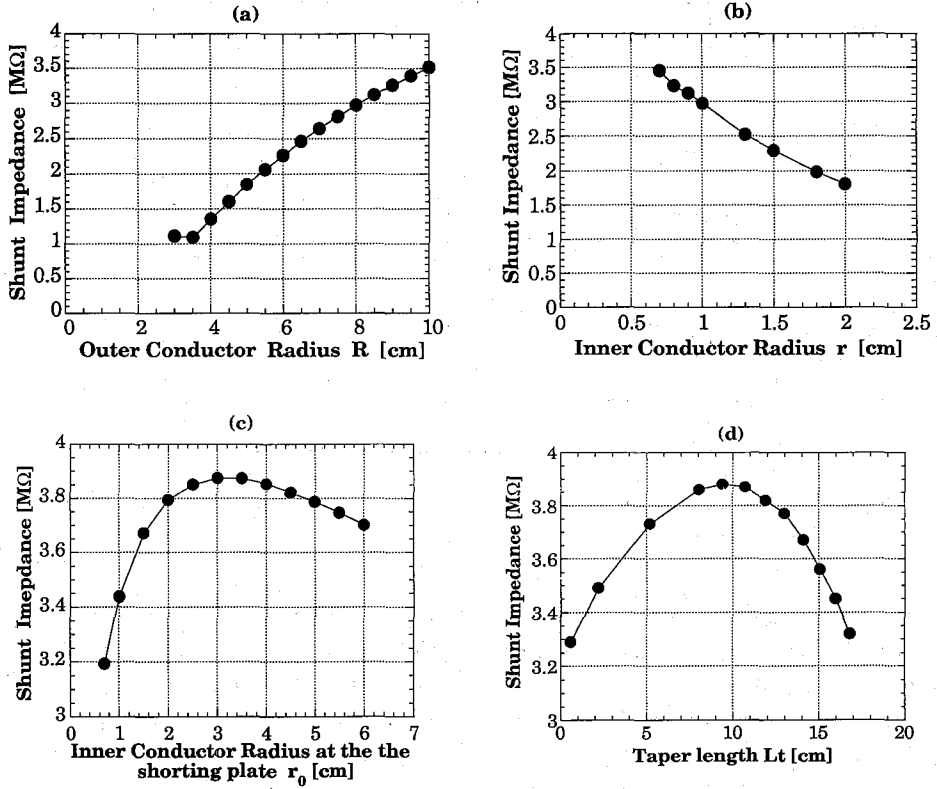


Fig. 5. (a) The shunt impedance of the buncher as a function of a internal radius of outer conductor,  $R$ . Both  $r$  and  $L_g$  are fixed at 10 mm. (b) The shunt impedance of the buncher as a function of a inner conductor radius  $r$ .  $R$  and  $L_g$  are fixed at 80 mm and 10 mm, respectively. (c) The shunt impedance of the buncher as a function of a inner conductor radius at the shorting plate  $r_0$ .  $R$  and  $r$  are set at optimized values of 8 cm and 0.7 cm, respectively. (d) The shunt impedance of the buncher as a function of the taper length  $L_t$ .  $R$  and  $r$  are set at optimized values of 8 cm and 0.7 cm, respectively.

presented in Fig. 6.

Figure 7 shows the changes of the effective shunt impedance  $ZT^2$  and the transit time factor with respect to the gap length  $L_g$ . As  $L_g$  becomes larger, the shunt impedance increases gradually while the transit time factor becomes smaller. As a result,  $ZT^2$  totally decreases with increasing  $L_g$ . Thus  $L_g$  is determined to be 5 mm. The shunt impedance of above design is 3.9  $M\Omega$  per gap.

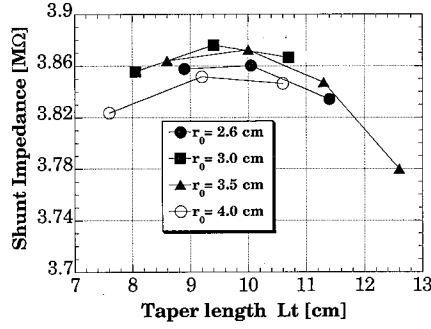


Fig. 6. The shunt impedance of the buncher as a function of the taper length  $L_g$  and inner conductor radius at shorting plate  $r_0$ .  $R$  and  $r$  are set at optimized values of 8 cm and 0.7 cm, respectively.  $L_g=9.4$  cm and  $r_0=3.0$  cm are the optimum point.

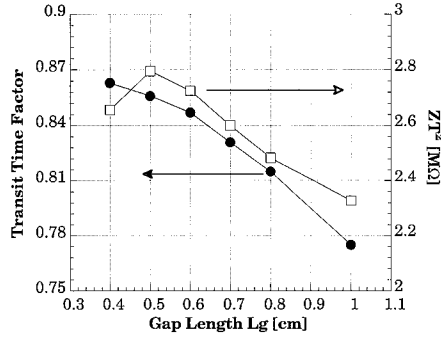


Fig. 7. The transit time factor and the effective shunt impedance as a function of gap length,  $L_g$ . Other parameters set at the optimized value are following,  $R=8.0$  cm,  $r=0.7$  cm,  $L_g=9.4$  cm,  $r_0=3.0$  cm.

#### 4. COLD MODEL MEASUREMENT

We fabricated a cold model of the designed buncher (Photo 1, and Photo 2). The shunt impedance  $Z$  of the model buncher can be evaluated by the measurements of  $Q$ -value and  $Z/Q$ . The loaded  $Q$  is given by

$$Q_L = \frac{f_0}{\Delta f}$$

where  $f_0$  is the resonant frequency and  $\Delta f$  is the half band width of the transmission. The frequency dependence of the transmitted power is shown in Fig. 8. The measured  $f_0$  was 413.11 MHz which was about 20 MHz lower than the designed frequency 433 MHz. This frequency difference would be mainly caused by the approximated geometry as mentioned before. The input coupling coefficient  $\beta$  was 1.15 while the output coupling coefficient was



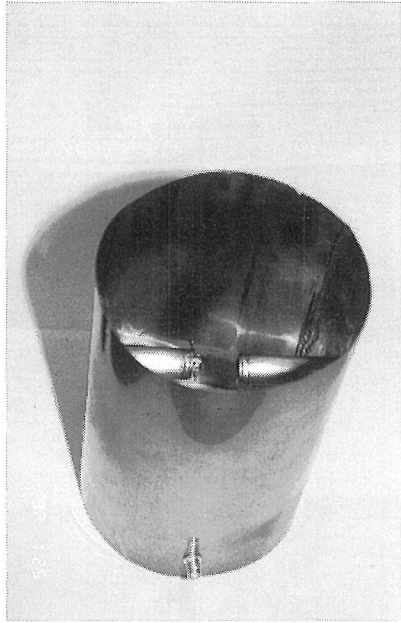


Photo. 1. The cold model of the buncher.

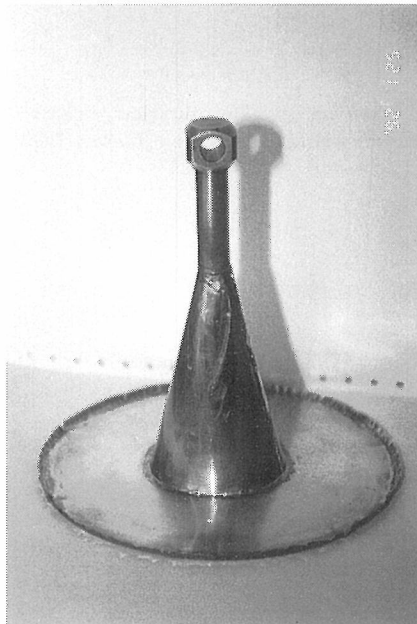


Photo. 2. The tapered inner conductor attached to the shorting plate.

# Design Study of a Beam Matching Section for the ICR Proton Linac

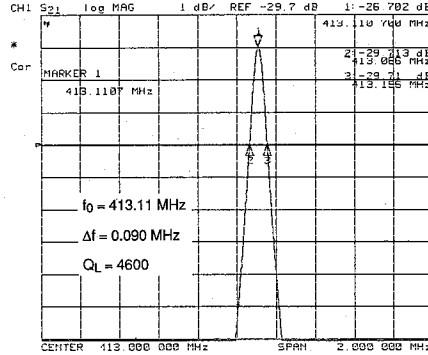


Fig. 8. The frequency dependence of the transmission power for the fabricated buncher.

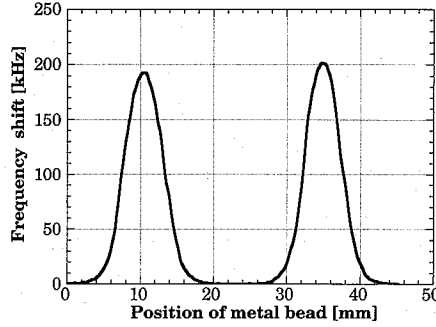


Fig. 9. The frequency shift along the beam axis by the bead-pull measurement.

found to be negligibly small. The unloaded  $Q$ , given by

$$Q = (1 + \beta) Q_L,$$

is 9800.

Figure 9 shows a result of the bead-pull measurement, where an aluminum bead of 1.2 mm radius was used. The data were taken at every 0.21 mm step along the beam axis.  $Z/Q$  is given by

$$\frac{Z}{Q} = \frac{4}{3\epsilon_0 \delta v \omega} \left( \int \sqrt{\frac{\Delta f}{f_0}} ds \right)^2$$

where  $\epsilon_0$  is the dielectric constant of vacuum,  $\delta v$  is the volume of the bead, and  $\omega$  is  $2\pi f_0$ . The obtained  $Z/Q$  and  $Z$  were 0.28 k $\Omega$  per gap, and 2.7 M $\Omega$  per gap, respectively. The required power  $P$  is calculated from

$$P = \frac{V_g^2}{Z}$$

where  $V_g$  is a specific gap voltage.

In the calculation of the longitudinal matching, the transit time factor and effective gap voltage are assumed to be 0.85 and 116 keV respectively. The specific gap voltage is calculated by

$$V_g = \frac{V_{eff}}{2T}$$

where  $V_{eff}$  is the effective gap voltage and the factor 2 comes from the double gap structure. The required RF power is 1700 W in order to generate the effective gap voltage needed in the longitudinal matching.

## 5. CONCLUSIONS

The optics of the beam matching section including four PMQ lenses and a buncher was optimized with the help of the computer code TRACE-3D. The optimized solution makes sure of the 100 % transmission rate which was confirmed with the PARMILA simulations.

The buncher geometry was also optimized with the use of the computer code SUPERFISH, though the resonant frequency of the model cavity was somewhat different from the expected frequency. The shunt impedance of the model cavity was measured to be 2.7 M $\Omega$  per gap which was 70 % of calculated value. We obtained a sufficient prospect to design a high shunt impedance buncher. The systematic procedure presented in this paper will be applied to design a real buncher cavity.

## REFERENCES

- 1) M. Sawamura et al.: "Design of 433.3MHz Alvarez Drift Tube Linac and Beam Matching Section", *Bull. Inst. Chem. Res. Kyoto Univ.*, Vol. 66, No. 1, 33-43, 1988.
- 2) I. Ben-Zvi and J. M. Brennan: "The Quarter Wave Resonator as a Superconducting Linac Element", *Nucl. Inst. and Meth.*, 212, 73-79 (1983).
- 3) D. W. Storm, J. F. Amsbaugh, D. T. Corcoran, and M. A. Howe: "Superconducting Tests of Beta = 0.1 and Beta = 0.2 Resonators", *Rev. Sci. Inst.* 57, (5), 733 (1986).
- 4) J. R. Delany: "Design of Low Velocity Superconducting Accelerating Structures Using Quarter-Wavelength Resonant Lines", *Nucl. Inst. and Meth.*, A259, 341-357 (1987).
- 5) S. Takeuchi, T. Ishii and H. Ikezoe: "Niobium Superconducting Quarter-wave Resonators as a Heavy Ion Accelerating Structure", *Nucl. Inst. and Meth.*, A281, 426-432 (1989).
- 6) K. Halbach and R. F. Holsinger: "SUPERFISH—A Computer Program for Evaluation of RF Cavity with Cylindrical Symmetry", *Particle Accelerators*, Vol. 7, 213-222 (1976).
- 7) K. R. Crandall: "TRACE 3-D documentation (second edition)", Los Alamos National Laboratory LA UR-90-4146.
- 8) K. R. Crandall, R. H. Stokes, and T. P. Wrangler: "RF Quadrupole Beam Dynamics Design Studies", 1979 Linear accelerator conference pp 205-216.
- 9) G. Boicourt and J. Merson: "PARMILA users and reference manual", published by Los Alamos National Laboratory 1990.